

3D Object Reconstruction Using Concatenated Matrices with MS Kinect: A Contribution to Interiors Architecture

Jorge Buele[1,4(✉)], José Varela-Aldás[1], Esteban X. Castellanos[2], Janio Jadán-Guerrero[1], and Jeneffer Barberán[3]

[1] SISAu Research Group, Universidad Tecnológica Indoamérica, Ambato 180212, Ecuador
{jorgebuele, josevarela, janiojadan}@uti.edu.ec
[2] Universidad de las Fuerzas Armadas ESPE, Latacunga 050104, Ecuador
excastellanos@espe.edu.ec
[3] Instituto Superior Tecnológico Tsa'chila, Santo Domingo 230109, Ecuador
jbarberan@institutos.gob.ec
[4] Universidad Internacional de la Rioja, 26006 Logroño, Spain

Abstract. Interior architecture is part of the individual, social and business life of the human being; it allows structuring the spaces to inhabit, study or work. This document presents the design and implementation of a system that allows the three-dimensional reconstruction of objects with a reduced economic investment. The image acquisition process and treatment of the information with mathematical support that it entails are described. The system involves an MS Kinect as a tool to create a radar that operates with the structured light principle to capture objects at a distance of less than 2 meters. The development of the scripts is done in the MATLAB software and in the same way the graphical interface that is presented to the user. As part of the initial tests of this prototype, the digitization of geometric shape structures has been performed with an accuracy of over 98%. This validates its efficient operation, which serves as the basis for the development of modeling in interior architecture for future work.

Keywords: 3D object reconstruction · Combined matrix · Image processing · Interior architecture · Software applications

1 Introduction

The three-dimensional digitization of objects is one of the applications of technology that is currently of greatest interest [1–3]. Various methodologies, procedures and techniques have been developed in the last three decades in order to obtain better representations [3]. Three-dimensional reconstruction is the process that allows user to form digital models in a computer, acquiring information (shape, volume, dimensions) of real objects [4]. This is to develop an algorithm that allows the connection of the set of representative points of an object in the form of surface elements with a geometric shape, such as squares, triangles, etc. The quality of the final product depends on the

© Springer Nature Switzerland AG 2020
O. Gervasi et al. (Eds.): ICCSA 2020, LNCS 12254, pp. 682–697, 2020.
https://doi.org/10.1007/978-3-030-58817-5_49

systematic fulfillment of the stages that make up the process, as well as an efficient representation of the set of points.

Among the most widely used methods based on optimal principles for acquiring 3D images are: holography, moiré, interferometry, radar, depth of focus and diffraction [5]. The radar system adopts its name from the acronym Radio Detection and Ranging, whose objective is to discover the presence of objects at a certain distance thanks to electromagnetic radiation [6]. If the electromagnetic waves are reflected on a conductive surface, they return to the point of emission and it can be inferred that an obstacle is found in the propagation path [7]. The delay and characteristics of this reflected signal serve the radar to determine the position, speed and even morphological properties of the body found. Using the structured light principle, a laser pulse is emitted; the distance of the object is obtained according to the deformation of the pattern, which can be: frequency bands or coded light [8].

This model can be one-dimensional or two-dimensional, in the case of one-dimensional it is a line which is projected onto the object with a laser, while the two-dimensional model is a grid, where a series of parallel vertical laser lines are considered that sweep horizontally the object. It has the advantage of speed, since it scans multiple points instead of one at a time, managing to analyze the entire field immediately [9]. Depth cameras that use the structured light method are RGB-D cameras, an example is the Microsoft Kinect device. These devices, in charge of capturing the data, combine hardware and software to produce an image based on a real object [10]. These images receive various names depending on the context where they are, which includes: scope image, depth image, range image, 3D image, list of XYZ points, among others [11]. Applications of these systems have diversified and are used by meteorologists to detect storms, hurricanes, and tornadoes, air traffic controllers to order airport traffic, NASA to create topographic maps of planets, and police to determine the speed at circulating vehicles [12].

2 Related Work

Several investigations have been carried out evidencing the use of radars in different fields of knowledge. In [11] a low-cost proposal that tries to supplant Mobile Terrestrial Laser Scanners (MTLS) for characterizing the geometry and structure of plants and crops for technical and scientific purposes has been done. Using a Kinect v2 depth sensor, a real-time kinematic Global Navigation Satellite System (GNSS) and a review of theoretical foundations, some experimental results are presented that illustrate its performance and limitations. Despite having a low measurement speed, plants, crops and other objects reproduce accurately. In aviation, unmanned aerial vehicles (UAVs) are used to perform visual assessments of infrastructure in real time, and the use of additional technology is required to evade obstacles. In [13], a study of the main tools for evading objects is presented, among them are radar systems. This study highlights the limitations that are found, since data acquired by the sensor is seriously affected by material deterioration of the structures that are being inspected.

In the technological field, radar systems are used for objects detection or the three-dimensional mapping of internal structures, as in [14]. Using two servo motors, a Light

Detection and Ranging (LIDAR) is moved and controlled in such a way that it measures the distance and angles simultaneously. This prototype has a simple and economical design, which wants to compete with devices that use the photogrammetry technique. They are sophisticated but often slow and expensive. Despite limitations of its design, it has good performance in terms of precision, reliability and cost-effectiveness. Mapping of underwater objects can also be done as proposed [15]. This work proposes the possibility of three-dimensional reconstruction of the surface of an underwater object that is at a certain depth. Images quality degrades and lighting is not uniform on the objects surface, just as the presence of particles in the water produces Gaussian noise. As a result, there is the reconstruction of 3D objects under water, but making some visual compensations in order to have significant savings in computational costs.

Gesture recognition using a MS Kinect device allows the design of an interactive tourist guide application, as can be seen in [16]. The design of an interactive tourist guide for visitors that recognizes gesture commands to show important information about shopping centers, restaurants, hotels and places of interest has been carried out. A MS Kinect-based user interface allows tourists to control the tour guide with movements of their hands, to preview images, data, and maps. This is a prototype system that will be implemented in a real environment to reinforce local and international tourism. In the case of interior architecture, [17] describes methods for recording work data using Kinect sensors. Various types of movements are registered in a construction, thereby enhancing the architectural area by managing sensors and cameras of this technological device.

Although the use of these commercial devices is wide, their application in architecture could open doors for greater and better applications that facilitate the work of designers, with decreasing investments. Therefore, this work presents a prototype system that allows the three-dimensional reconstruction of objects in the field of low-cost interior architecture. The acquisition of images is carried out using the Kinect device, whose information is transferred to the MATLAB mathematical software. The mathematical process that must be considered before the development of the respective scripts that manage the subsequent digitization of the objects has been described. As well as the tests that demonstrate its operation and are used to determine its accuracy. This article is organized as follows: the introduction in Sect. 1, Sect. 2 shows the state of the art. In Sect. 3 the image acquisition is presented while in Sect. 4 the development of the proposal is detailed. The results of the experimental tests carried out and conclusions are described in Sect. 5 and Sect. 6 respectively.

3 Image Acquisition

3.1 Object Detection

The object is detected by emitting a signal from the Kinect's infrared sensor that manages to reflect itself after colliding with the object in question; this signal produces a modulation of a cosine function, as shown in (1). The wave is a function of time and the sampling frequency where (V_0) is the propagation speed, in which case it refers to

the speed of light to be emitted from the Kinect's infrared sensor, (*f*) is the frequency of the transmitted signal, (*t*) the time and (φ_0) the phase angle. It must be taken into account that there is a time delay due to the emission and reflection of the wave, which in turn produces an offset, this generates Eq. (2) as a reference for the correct detection of the object.

$$V(t) = V_0 \cos(2\pi f_t + \varphi_0) \tag{1}$$

$$V_r(t) = V_0 K \cos(2\pi f(t - 2t_r) + \varphi_0)\, \mu(t - 2t_r) \tag{2}$$

3.2 Object Distance

Once the object is detected, it is necessary to know the distance at which it is located, so the Chirp signal that changes from low to high frequency or vice versa within a defined period of time is analyzed. The variant frequency in time $f(t)$ depends on the speed with which the frequency k changes, where the initial frequency of the wave f_0 and final frequency f_1 are taken into account for a duration T, thus obtaining (3) and (4) that by replacing data in (2), we finally obtain (5), where both the angle offset and the time delay of the signal are already considered. By using the Fast Fourier Transform (FFT) the distance at which the object was found is determined at the highest peak.

$$f(t) = \frac{k}{2}t + f_0 \tag{3}$$

$$k = \frac{f_1 - f_0}{T} \tag{4}$$

$$V_r(t) = V_0 K \cos\left(2\pi\left(\frac{k}{2}(t - 2t_r) + f_0\right)(t - 2t_r) + \varphi_0\right)\mu(t - 2t_r) \tag{5}$$

3.3 System Resolution

The resolution of the system is the ability to determine the minimum distance located between two objects whose characteristics are analogous; that is why the resolution is mathematically defined as the accuracy of the distance (e_d), shown in (6); whose value is found as a function of the wave propagation speed, defined as the speed of light (c) and the bandwidth (B) that is determined by the doubling of the maximum frequency of the system.

$$\Delta R = e_d = \frac{c}{B} = \frac{c}{2 * f_{\max}} \tag{6}$$

4 Development of the Proposal

4.1 Hardware

The proposal presented by the authors of the work is based on the interconnection of a personal computer (PC) with the MS Kinect device using software that expands compatibility, such as Open NI, for data extraction, and MATLAB for data processing. The minimum specifications of the PC lie in the possibility of processing images at high speeds without meaning a high economic cost, so in this proposal a PC with 8 GB of DDR4 RAM (Double Data Rate version 4), 4 GB of memory was used for a dedicated GDDR5 (Graphics Double Data Rate version 5) video card and a USB 3.0 port for obtaining data from the technology device as soon as possible.

Regarding the MS Kinect, the device with version 2.0 was used, which allows the detection of more objects with a better resolution. This translates into greater sensitivity in its CMOS emitters and receivers. The operation of the device is based on the emission of infrared signals that bounce off an object following a pattern of points that later return to the infrared CMOS receiver, as each signal bounces, the presence of an object or part of it is assumed. In Fig. 1 it can be seen the general scheme of the system that has a high portability index due to its low weight by the elements involved in it.

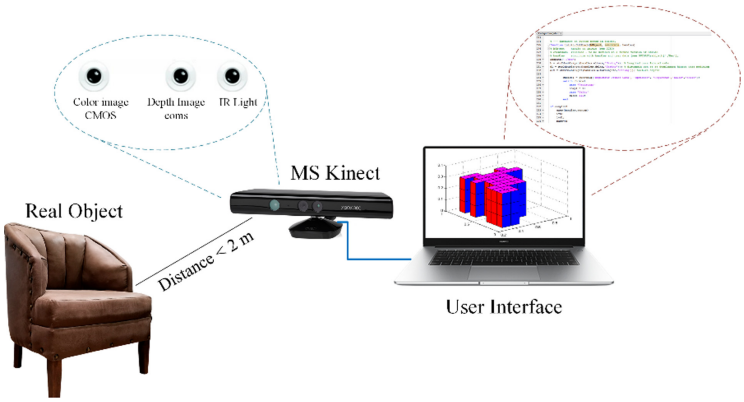

Fig. 1. General scheme of the system.

4.2 MATLAB Script

The initial part is the download and installation of the Open NI libraries, NITE PrimeSense and the MEX files that allow linking the Kinect device with the MATLAB software. The Open NI library provides a generic infrastructure based on open source APIs to access and control the Kinect accessories: camera, sensor and audio. The NITE

library, whose code is not open, is used to access advanced device functionalities, such as tracking an object in real time. For the interaction between the device and the software, open source MEX files implemented by developers on the web have been used. These files are called Kinect-Mex and allow the necessary information to be obtained from the images regarding depth, RGB and infrared.

To establish the link, add the path of the folder where the MEX files are located, whose files allow to turn the device on and off, as well as access its operating modes. Through the "mxNiCreateContex" function, the SamplesConfig.xml operation mode is enabled, it allows to obtain both RGB and depth images at a resolution of 640 x 480 pixels (this structure will be kept by default from now on). The colour image information must be aligned with the depth image because the infrared camera is not in the same position as the RGB camera, so the images are offset from each other. RGB image information is stored in one variable and depth image information in another.

4.3 Selection of Information and Storage

The information obtained by default in Kinect is represented in pixels (u, v) for this reason the depth values must be transformed to units of length (mm). To obtain the distance of the object from the device, the depth image information is selected at a specific point. For this, coordinates that will select data location in the real_XYZ matrix are added, being of a special interest the central data of the image, as can be seen in Fig. 2. To store the information of each side face of the cube that covers the object, certain parameters are defined such as: height of the object (alt), distance that each measurement will be taken vertically (dlv), length of the horizontal edge (h) and the distance to which each measurement will be taken horizontally (dl). Its graphic representation can be seen in Fig. 2.

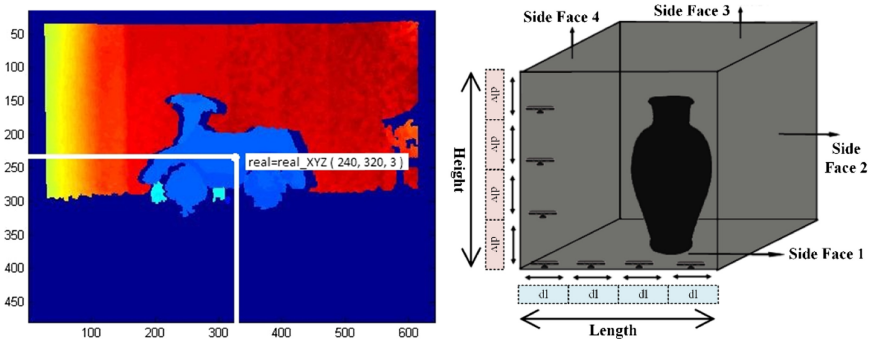

Fig. 2. Image Information of central data (Left). 3D Reconstruction parameters (Right).

The information stored in the variable real_XYZ is used each time the distance measurement is carried out for horizontal and vertical movements. To store all measurements made of one of the lateral faces in a vector, a repeating structure is used to cover the entire lateral face making a horizontal and vertical sweep. The distance at which the Kinect object is located is stored in the variable real_XYZ (240,320.3) in pixels and to obtain said distance in millimeters it is divided by 1000.

Real depth of an object is obtained with the difference between real_XYZ (240, 320, 3) and the length of the horizontal edge. On the other hand, if the horizontal edge length is less than the variable real_XYZ (240,320.3), the depth reminds to zero because no object is found for that location. This procedure is described in Algorithm 1.

Algorithm 1. Repetition structure used to cover the entire side face.

```
i=0;
base=0;
heightob=0;
range=h/dl; % Data number per row
rangealt=alt/dlv; % Row number
contalt=1;
cont=1;
while (base<= range && alturaob <= rangealt)
i=i+1;
real= (real_XYZ(240,320,3)/1000); %Profundity data
if (real<=h && real~=0)
   y(i)=h-real; % Distance data
   else
   y(i)=0;
end
    cont=cont+1;
    base=cont;
if (base>range && heightob<rangealt)
         cont=1;
          l=dl;
          base=0;
          contalt=contalt+1;
          heightob=contalt;
                end
end
```

Once measurements are stored in the vector, said vector is converted into a matrix, for this the mathematical expressions described in (7) and (8) are used and thus dimensions of the matrix are determined. Where m = number of rows in the matrix, c = number of columns in the matrix, A = stored vector and M = information matrix.

$$m = \frac{alt}{dlv} \tag{7}$$

$$c = \frac{h}{dl} \tag{8}$$

4.4 Reconstruction of the 3D Object

Creation of Matrices 0's. Once matrices that store the depth measurements of the four lateral faces are obtained, four square matrices of 0's are created with a dimension equal to the number of columns that one of the stored matrices has, as expressed in (8). Thus, each data in a row of the depth matrix is related to a column of the 0's matrix, so that 1's is assigned in each column of the 0's matrix according to the value of the data in the row of the matrix of depth. The face 1 data matrix is presented in (9) and filled with zeros. Following the same principle, the matrices of the remaining faces (B (m × c), C (m × c) and D (m × c)) are defined.

$$A_{(mxc)} = \begin{pmatrix} a_{1,1} & a_{1,2} & a_{1,3} & \cdots & a_{1,c} \\ a_{2,1} & a_{2,2} & a_{2,3} & \cdots & a_{2,c} \\ a_{3,1} & a_{3,2} & a_{3,3} & \cdots & a_{3,c} \\ \vdots & \vdots & \vdots & \vdots & \vdots \\ a_{m,1} & a_{m,2} & a_{m,3} & \cdots & a_{m,c} \end{pmatrix} \tag{9}$$

Depth of an Object Represented in 1's. To assign 1's to the 0's matrices (10) is used, which determines the number of 1's that will be replaced in each column. This equation is used for all data in a row of the stored matrices. p1 is the number of 1 s representing the object distance from the Kinect location for matrix data A (1, j). Following the same principle, matrices 0's are defined for the other three remaining faces with data from matrices B (1, j) (p2), C (1, j) (p3) and D (1, j) (p4). Both p1 and p2, p3, and p4 must be integers. This process is described in Algorithm 2 and the respective 1's matrix is presented in (11).

$$p_1 = \frac{A(a_{1,j}) * c}{h} \tag{10}$$

$$\begin{cases} C1A_{i,j} = 1,\ i \geq p_1 \\ C1A_{i,j} = 0,\ i < p_1 \end{cases} \quad \forall i,j = 1,2,\ldots,c$$

$$C1A_{(cxc)} = \begin{pmatrix} 1_{1,1} & 1_{1,2} & 1_{1,3} & \cdots & 1_{1,c} \\ 1_{2,1} & 1_{2,2} & 1_{2,3} & \cdots & 1_{2,c} \\ \vdots & \vdots & \vdots & \vdots & \vdots \\ 1_{(p),1} & 1_{(p),2} & 1_{(p),3} & \cdots & 1_{(p),c} \\ 0_{(p+1),1} & 0_{(p+1),2} & 0_{(p+1),3} & \cdots & 0_{(p+1),c} \\ \vdots & \vdots & \vdots & \ddots & \vdots \\ 0_{c,1} & 0_{c,2} & 0_{c,3} & \cdots & 0_{c,c} \end{pmatrix} \tag{11}$$

Algorithm 2. Definition of 0s matrices for whole four faces

```
cuad=(columns);
matcerosc1=zeros(cuad); %0's para Face 1
matcerosc2=zeros(cuad); %0's para Face 2
matcerosc3=zeros(cuad); %0's para Face 3
matcerosc4=zeros(cuad); %0's para Face 4
    for i=1:columns
     posc1= t1(controws,i); %Side Face 1
     posc11=((posc1*cuad)/h);
     posc111=round(posc11);
     posc2= t2(controws,i); %Side Face 2
     posc22=((posc2*cuad)/h);
     posc222=round(posc22);
     posc3=t3(controws,i); %Side Face 3
     posc33=((posc3*cuad)/h);
     posc333=round(posc33);
     posc4= t4(controws,i); %Side Face 4
     posc44=((posc4*cuad)/h);
     posc444=round(posc44);
        for j=1:posc111
         matzerosc1(j,i)=1;
        end
        for j=1:posc222
         matzerosc2(j,i)=1;
        end
        for j=1:posc333
         matzerosc3(j,i)=1;
        end
        for j=1:posc444
         matzerosc4(j,i)=1;
        end     end
```

Assigning 1's in the matrices of 0's for data of one of the rows of the matrices that keep the depth measurements. To continue with the process, rotations are made to the matrices of 1's according to the order of how depth measurements of the object are taken, which may be hourly or anti-hourly. Next, it should be performed the position by position multiplication type of the matrices 0's, obtaining as a result a matrix where the object is reconstructed in a flat way for row 1 of the matrices A, B, C and D. Finally, in order to obtain the object in 3D, the resulting matrix is graphed using the boxplot3 function. To reconstruct an object with n rows of information, a repeating structure must be followed to reuse matrices 0´s and assign 1´s for each row of information in matrices A, B, C and D, being m the number of rows which contains each information matrix stored as described in (12).

$$R_{(cxcxm)} = \text{ref}\left(\text{ref}\left(A(i.j)^T\right)\right)^T x\text{ref}\left(B(i.j)^T\right)xC(i.j)x(\text{ref}(D(i.j)))^T \tag{12}$$

5 Result Analysis

5.1 Original Matrices

Based on technical features of the MS Kinect, it is recommended to locate the objects at a maximum distance of 2 m, without loss of information or confusion in the process. Several tests were carried out with rectangular geometric objects of different sizes, simulating the presence of typical objects from an architectural space. For the presentation of results, only one test has been taken as a reference, to test the correct operation and determine the parameters that must be considered. For this case, a horizontal displacement of 0.2 m, vertical displacement of 0.2 m and a height of 0.2 m have been established. In the reconstruction of objects, it is defined that each data with value "1" represents a fraction of the object that is located in an imaginary hexahedron or cube for the data set that contains the binary matrix.

Once matrices that store depth measurements of the four lateral faces are obtained, four 0's square matrices are created with a dimension equal to the number of columns that one of the stored matrices has. Once the system has determined the number of 1's that will be located in the 0's matrices and the result has been rounded, the Values of the stored data matrices are obtained as shown in Table 1 (row 1) and Table 2 (row 2). In Fig. 3 shows the matrices obtained and in Fig. 4 their reconstruction presented in the designed interface. In Fig. 4 the reconstruction of the same object from another point of view is evidenced.

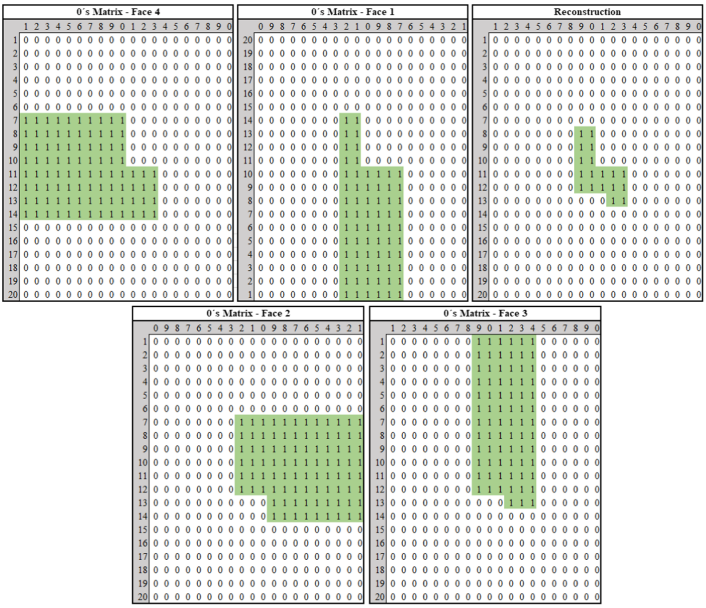

Fig. 3. 0's matrices (4 faces and reconstruction) with 1's assignment.

Table 1. 4-sided reconstruction matrix: Row 1

Item	Face 1 matrix			Face 2 matrix			Face 3 matrix			Face 4 matrix		
	M	R3	1's	M	R3	1's	M	R3	1's	M	R3	1's
(1.1)	0	0	0	0	0	0	0	0	0	0	0	0
(1.2)	0	0	0	0	0	0	0	0	0	0	0	0
(1.3)	0	0	0	0	0	0	0	0	0	0	0	0
(1.4)	0	0	0	0	0	0	0	0	0	0	0	0
(1.5)	0	0	0	0	0	0	0	0	0	0	0	0
(1.6)	0	0	0	0	0	0	0	0	0	0	0	0
(1.7)	0,993	9,93	10	1,181	11,81	12	0	0	0	1,309	13,09	13
(1.8)	0,994	9,94	10	1,181	11,81	12	0	0	0	1,309	13,09	13
(1.9)	0,993	9,93	10	1,179	11,79	12	1,182	11,82	12	1,31	13,1	13
(1.10)	0,994	9,94	10	1,18	11,8	12	1,188	11,88	12	1,301	13,01	13
(1.11)	1,313	13,13	13	1,181	11,81	12	1,181	11,81	12	1,017	10,17	10
(1.12)	1,309	13,09	13	1,18	11,8	12	1,181	11,81	12	1,017	10,17	10
(1.13)	0	0	0	0,884	8,84	9	1,317	13,17	13	1,012	10,12	10
(1.14)	0	0	6	0,88	8,8	9	1,318	13,18	13	1,012	10,12	10
(1.15)	0	0	0	0	0	0	0	0	0	0	0	0
(1.16)	0	0	0	0	0	0	0	0	0	0	0	0
(1.17)	0	0	0	0	0	0	0	0	0	0	0	0
(1.18)	0	0	0	0	0	0	0	0	0	0	0	0
(1.19)	0	0	0	0	0	0	0	0	0	0	0	0
(1.20)	0	0	0	0	0	0	0	0	0	0	0	0

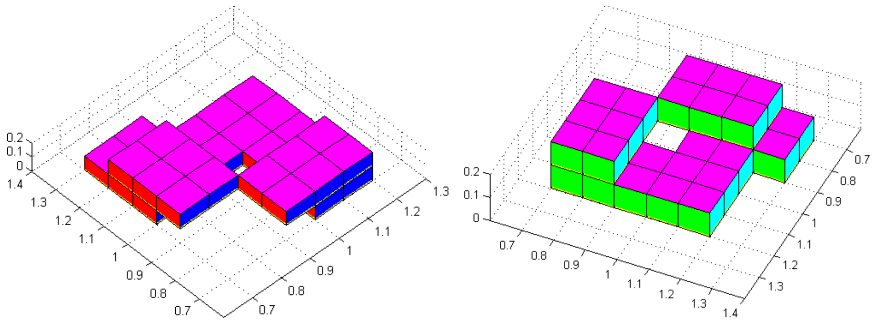

Fig. 4. Three-dimensional reconstruction of: First set of objects (Left). Other view (Right).

Table 2. 4-sided reconstruction matrix: Row 2

Item	Face 1 matrix			Face 2 matrix			Face 3 matrix			Face 4 matrix		
	M	R3	1's	M	R3	1's	M	R3	1's	M	R3	1's
(2.1)	0	0	0	0	0	0	0	0	0	0	0	0
(2.2)	0	0	0	0	0	0	0	0	0	0	0	0
(2.3)	0	0	0	0	0	0	0	0	0	0	0	0
(2.4)	0	0	0	0	0	0	0	0	0	0	0	0
(2.5)	0	0	0	0	0	0	0	0	0	0	0	0
(2.6)	0	0	0	0	0	0	0	0	0	0	0	0
(2.7)	0	0	0	1,208	12,08	12	0	0	0	0	0	0
(2.8)	1,138	11,81	11	1,208	12,08	12	0	0	0	0	0	0
(2.9)	1,138	11,81	11	1,21	12,1	12	0,85	8,5	9	1,288	12,88	13
(2.10)	1,35	9,94	13	0,912	9,12	9	0,85	8,5	9	1,287	12,87	13
(2.11)	1,35	13,13	13	0,912	9,12	9	0,85	8,5	9	1,287	12,87	13
(2.12)	1335	13,09	13	0,92	9,2	9	1,148	11,5	12	1,08	10,8	11
(2.13)	0	0	0	0	0	0	1,148	11,51	12	1,08	10,8	11
(2.14)	0	0	6	0	0	0	0	0	0	1,08	10,8	11
(2.15)	0	0	0	0	0	0	0	0	0	0	0	0
(2.16)	0	0	0	0	0	0	0	0	0	0	0	0
(2.17)	0	0	0	0	0	0	0	0	0	0	0	0
(2.18)	0	0	0	0	0	0	0	0	0	0	0	0
(2.19)	0	0	0	0	0	0	0	0	0	0	0	0
(2.20)	0	0	0	0	0	0	0	0	0	0	0	0

5.2 Concatenated Matrices

After obtaining the first results in previous works that were not completely satisfactory, the design of an algorithm is proposed in this research to dimension each data of the information matrices of the object lateral faces [18]. This is needed in order to obtain each dimensioned data to a sub-matrix of (5 * 5) by resizing the information matrices to (n * 5) × (m * 5). Resizing will allow curvilinear objects to be 3D reconstructed similarly to the real object. In (13) there is a normal matrix and in (14) the same matrix is obtained, but this time it is concatenated. To demonstrate the operation of the objects reconstruction in three-dimensional form with concatenated data from the measurements made on the lateral faces, the same objects previously tested were reconstructed exposing the results below. Figure 5 shows the results obtained.

$$A = \begin{pmatrix} aa_{1,1} & ab_{1,2} & \cdots & az_{1,m} \\ ba_{2,1} & bb_{2,2} & \cdots & bz_{2,m} \\ \vdots & \vdots & \ddots & \vdots \\ za_{n,1} & zb_{n,2} & \cdots & zz_{n,m} \end{pmatrix} \tag{13}$$

$$AC = \begin{pmatrix} \begin{pmatrix} aa_{1,1} & \cdots & aa_{1,5} \\ \vdots & \ddots & \vdots \\ aa_{5,1} & \cdots & aa_{5,5} \end{pmatrix}_{1,1} & \begin{pmatrix} ab_{1,1} & \cdots & ab_{1,5} \\ \vdots & \ddots & \vdots \\ ab_{5,1} & \cdots & ab_{5,5} \end{pmatrix}_{1,2} & \cdots & \begin{pmatrix} az_{1,1} & \cdots & az_{1,5} \\ \vdots & \ddots & \vdots \\ az_{5,1} & \cdots & az_{5,5} \end{pmatrix}_{1,m} \\ \begin{pmatrix} ba_{1,1} & \cdots & ba_{1,5} \\ \vdots & \ddots & \vdots \\ ba_{5,1} & \cdots & ba_{5,5} \end{pmatrix}_{2,1} & \begin{pmatrix} bb_{1,1} & \cdots & bb_{1,5} \\ \vdots & \ddots & \vdots \\ bb_{5,1} & \cdots & bb_{5,5} \end{pmatrix}_{2,2} & \cdots & \begin{pmatrix} bz_{1,1} & \cdots & bz_{1,5} \\ \vdots & \ddots & \vdots \\ bz_{5,1} & \cdots & bz_{5,5} \end{pmatrix}_{2,m} \\ \vdots & \vdots & \ddots & \vdots \\ \begin{pmatrix} za_{1,1} & \cdots & za_{1,5} \\ \vdots & \ddots & \vdots \\ za_{5,1} & \cdots & za_{5,5} \end{pmatrix}_{n,1} & \begin{pmatrix} zb_{1,1} & \cdots & zb_{1,5} \\ \vdots & \ddots & \vdots \\ zb_{5,1} & \cdots & zb_{5,5} \end{pmatrix}_{n,2} & \cdots & \begin{pmatrix} zz_{1,1} & \cdots & zz_{1,5} \\ \vdots & \ddots & \vdots \\ zz_{5,1} & \cdots & zz_{5,5} \end{pmatrix}_{n,m} \end{pmatrix}_{((n*5)x(m*5))} \tag{14}$$

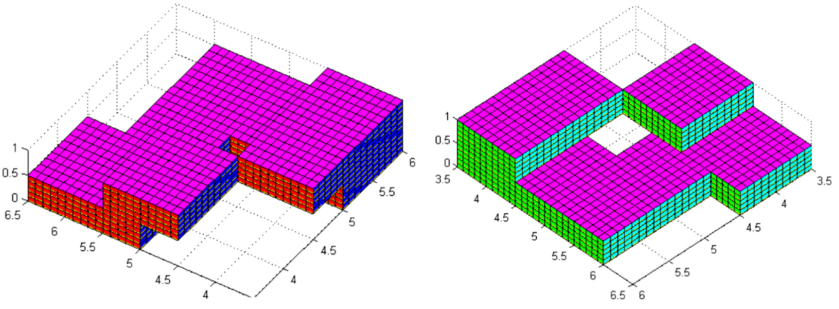

Fig. 5. 3D reconstruction of the object with concatenated data.

5.3 System Precision and Accuracy

To determine the depth data obtained accuracy, 20 experimental measurements were taken as a sample on an object located approximately 150 cm away. 10 ascending displacements with an interval of 20 cm and 10 descending displacements of the same value. All measures were taken to obtain the true error of each data and the mean of the relative percentage error of the data using (15). Where (Ev) is the true error and (Et) is the percentage relative error. Table 3 shows the actual depth data and those obtained in the measurements, expressed in millimeters and each of the previously mentioned errors.

$$\bar{E}t = \frac{Et_1 + Et_2 + Et_3 + \ldots + Et_n}{n} \tag{15}$$

Table 3. Depth errors.

Real	Measured	Ev	Et	Et(%)	Real	Measured	Ev	Et	Et(%)
1500	1517	17	0,011	1,13%	1480	1497	17	0,011	1,15%
1520	1538	18	0,012	1,18%	1460	1474	14	0,010	0,96%
1540	1557	17	0,011	1,10%	1440	1460	20	0,014	1,39%
1560	1578	18	0,012	1,15%	1420	1441	21	0,015	1,48%
1580	1598	18	0,011	1,14%	1400	1416	18	0,013	1,29%
1600	1617	17	0,011	1,06%	1380	1396	16	0,012	1,16%
1620	1641	21	0,013	1,30%	1360	1377	17	0,013	1,25%
1640	1667	27	0,016	1,65%	1340	1355	15	0,011	1,12%
1660	1685	25	0,015	1,51%	1320	1340	20	0,015	1,52%
1680	1711	31	0,018	1,85%	1300	1314	14	0,011	1,08%

Now, the accuracy is defined as how close is the measured value from the true value, so that for the measurements shown in Table 3, the accuracy with which a depth data is obtained is determined to be about 3 mm. Considering the mean of the relative percentage error (1.27%), it is determined that its difference expresses 98.73% of precision, for when the IR and RGB cameras are located at an angle parallel to the ground.

World current landscape involves digitization tasks, object reconstruction with high precision and task execution using gestures [14–16]. This proposal emphasizes a good content as well as less investment in resources. At this time, the economy in Latin America is not the most advantageous, so researchers are currently seeking to achieve great objectives by innovating methods that ensure functionality using low-cost tools. Thus, while [17] reconstruct an environment by mapping in 3D, it does not meet the precision needs for using the reconstructed model in design applications. Despite its reduced cost, it could not have an application that involves interior architecture as presented in this manuscript.

6 Conclusions

The applications presented by radar systems are multiple, as evidenced in the presented bibliography. The use of technology to establish new and better tools for interior space designers has motivated the development of this research as a low-cost proposal. The technical specifications of the Kinect applied to this application have determined that the angle of inclination of the infrared and photogrammetric camera is not more than 30° maximum down and up. The neutral position is when device is parallel to the ground, but 10 other different positions can also be programmed. Despite this, it has not been necessary to use them and the neutral position has been maintained with the intention of not accidentally modifying the data obtained. Tests carried out on previous prototypes were not satisfactory and after some modifications and considerations it has been determined that the minimum depth of an object is 89 cm and a maximum of 192 cm.

The initial object reconstruction presented results with insufficient definition and therefore it was necessary to apply concatenated matrices that allow better information processing to improve results. A sample of different measurements was taken while the experimental tests were carried out, and an accuracy of 98.73% was obtained when operating within the proposed depth range. Increasing this measurement, certain parts of the object were not properly reconstructed. During the experimental stage, geometric figures have been used, since they have facilitated the calibration and adjustment of the system. Feedback obtained during the development of this research will allow future improvements in the design of the third version of this prototype. In this way, it has been possible to demonstrate its correct operation and establish it as a valid technological tool to improve the interior environment design that professionals use to optimize their time at a low cost.

Authors propose as future work to improve this design and to carry out more detailed tests with other elements that are part of architectural interiors. Also test its application in other fields of science and be able to make a comparison of results obtained. This will allow to enrich the design of new technological instruments that seek to improve the quality of life of the human being.

Acknowledgments. A special thanks to the Universidad Tecnológica Indoamérica for supporting the development of this work.

References

1. Fernández-S, Á., Salazar-L, F., Jurado, M., Castellanos, E.X., Moreno-P, R., Buele, J.: Electronic system for the detection of chicken eggs suitable for incubation through image processing. In: Rocha, Á., Adeli, H., Reis, L.P., Costanzo, S. (eds.) WorldCIST'19 2019. AISC, vol. 931, pp. 208–218. Springer, Cham (2019). https://doi.org/10.1007/978-3-030-16184-2_21
2. Hugeng, H., Anggara, J., Gunawan, D.: Implementation of 3D HRTF interpolation in synthesizing virtual 3D moving sound. Int. J. Technol. (2017). https://doi.org/10.14716/ijtech.v8i1.6859

3. Elsayed, M., Soe, M.T., Kit, W.W., Abdalla, H.: An innovative approach to developing a 3D virtual map creator using an ultrasonic sensor array. Int. J. Technol. (2019). https://doi.org/10.14716/ijtech.v10i7.3245
4. Protasov, A.: Active infrared testing of composites using 3D computer simulation. Int. J. Technol. (2018). https://doi.org/10.14716/ijtech.v9i3.218
5. Taylor, M.: Lifshitz holography. Class. Quantum Gravity (2016). https://doi.org/10.1088/0264-9381/33/3/033001
6. Chiani, M., Giorgetti, A., Paolini, E.: Sensor Radar for object tracking (2018). https://doi.org/10.1109/JPROC.2018.2819697
7. Meinl, F., Stolz, M., Kunert, M., Blume, H.: An experimental high performance radar system for highly automated driving. In: 2017 IEEE MTT-S International Conference on Microwaves for Intelligent Mobility, ICMIM 2017 (2017). https://doi.org/10.1109/ICMIM.2017.7918859
8. Moreno Avilés, D., Mejía, J., Moreno, H.: Desarrollo de un algoritmo en MATLAB para la optimización de la resolución de una tarjeta USRP B210 para aplicaciones SDRadar. MASKAY (2017). https://doi.org/10.24133/maskay.v7i1.338
9. Iakushkin, O., Selivanov, D., Tazieva, L., Fatkina, A., Grishkin, V., Uteshev, A.: 3D reconstruction of landscape models and archaeological objects based on photo and video materials. In: Gervasi, O., et al. (eds.) ICCSA 2018. LNCS, vol. 10963, pp. 160–169. Springer, Cham (2018). https://doi.org/10.1007/978-3-319-95171-3_14
10. Capece, N., Erra, U., Romaniello, G.: A low-cost full body tracking system in virtual reality based on microsoft kinect. In: De Paolis, L.T., Bourdot, P. (eds.) AVR 2018. LNCS, vol. 10851, pp. 623–635. Springer, Cham (2018). https://doi.org/10.1007/978-3-319-95282-6_44
11. Rosell-Polo, J.R., et al..: Kinect v2 sensor-based mobile terrestrial laser scanner for agricultural outdoor applications. IEEE/ASME Trans. Mechatron. (2017). https://doi.org/10.1109/TMECH.2017.2663436
12. Pritchard, M.E., Yun, S.-H.: Satellite radar imaging and its application to natural hazards. In: Natural Hazards (2018). https://doi.org/10.1201/9781315166841-5
13. Jordan, S., et al.: State-of-the-art technologies for UAV inspections, (2018). https://doi.org/10.1049/iet-rsn.2017.0251
14. Riaz, M., Bukhari, S.A., Mukhtar, F., Kamal, T., Sarwar, H., Tahir, M.U.: 3D mapping using light detection and ranging. In: Proceedings of 2017 International Multi-Topic Conference, INMIC 2017 (2018). https://doi.org/10.1109/INMIC.2017.8289468
15. Anwer, A., Ali, S.S.A., Meriaudeau, F.: Underwater online 3D mapping and scene reconstruction using low cost kinect RGB-D sensor. In: International Conference on Intelligent and Advanced Systems, ICIAS 2016 (2017). https://doi.org/10.1109/ICIAS.2016.7824132
16. Minda Gilces, D., Matamoros Torres, K.: A kinect-based gesture recognition approach for the design of an interactive tourism guide application. In: Communications in Computer and Information Science (2018)
17. Ishida, K.: Construction progress management and interior work analysis using kinect 3D image sensors. In: ISARC 2016 - 33rd International Symposium on Automation and Robotics in Construction (2016)
18. Barberán, J., et al.: Radar system for the reconstruction of 3D objects: a preliminary study. In: Rocha, Á., Adeli, H., Reis, L.P., Costanzo, S., Orovic, I., Moreira, F. (eds.) WorldCIST 2020. AISC, vol. 1160, pp. 238–247. Springer, Cham (2020). https://doi.org/10.1007/978-3-030-45691-7_23